Waste Management 181 (2024) 101–113

Contents lists available at ScienceDirect

Waste Management

journal homepage: www.elsevier.com/locate/wasman

Research Paper

The relevant effect of marine salt and epiphytes on *Posidonia oceanica* waste pyrolysis: Removal of SO_2/HCl emissions and promotion of O/HCOOH formation

M.B. Folgueras [a], Antonio J. Gutiérrez-Trashorras [b], G. Laine-Cuervo [a], Juan Carlos Ríos-Fernández [a,b,*]

[a] Department of Energy, University of Oviedo, Polytechnic School of Mieres, c/ Gonzalo Gutiérrez Quirós s/n, 33600 Mieres, Asturias, Spain
[b] Department of Energy, University of Oviedo, Polytechnic School of Engineering of Gijón, Campus de Viesques, 33203 Gijón, Asturias, Spain

ARTICLE INFO

Keywords:
Posidonia oceanica waste
Pyrolysis
Carbonates
Formic acid
Char gasification
Atomic oxygen

ABSTRACT

Significant quantities of *Posidonia oceanica* deposit on some beaches and coastlines every year, which generates high costs associated with the disposal of this waste. Pyrolysis may be an adequate way for its valorization. However, it would imply to know how the process takes place and if the removal of its natural detrital inorganic matter (epiphytes, marine salt and sand) is necessary, which are the objectives of this research. Pyrolysis by thermogravimetry-mass spectrometry was carried out on both the washed and unwashed samples.

During this waste pyrolysis, the following occurs: (i) the high alkali metal chloride content promotes fragmentation reactions of carbohydrates and O formation, which increases HCOOH intensities at temperatures between 250 and 360 °C; (ii) from 500 °C to 650 °C, Fe_2O_3 and decomposition of carbonates seem to be involved in reactions that produce O release and steam and CO_2 reforming of hydrocarbons and oxygenated organic compounds with H_2 generation; (iii) from 650 °C to 750 °C, Fe_2O_3, high alkali metal content and carbonate decomposition generate char gasification, an increase in O release, SO_2 capture and HCOOH formation.

In general, the abundance of inorganic matter (chlorides, carbonates, etc.) minimizes the release of various compounds during pyrolysis, including SO_2 and HCl, while increasing HCOOH production. Thus, this high content of inorganic matter may represent an advantage for its pyrolysis, producing value-added chemical products with a reduced environmental impact. Therefore, this study may be the starting point for defining the optimal pyrolysis conditions for this waste valorisation.

Nomenclature

Symbols/abbreviations	
A	Ash
AAEM	Alkali and alkaline earth metals
$C_{carbonates}$	Carbon from carbonates
C_{org}	Organic carbon
CELL	Cellulose
CY	Carbon yield
DTG	Derivative TG
HCELL	Hemicellulose
HHV	Higher heating value
FC	Fixed carbon
IC	Inorganic carbon

(*continued on next column*)

Nomenclature (*continued*)

Symbols/abbreviations	
ICP	Inductively Coupled Plasma
IDA	Isotope Dilution Analysis
LIG	Lignin
m/z	Mass-to-charge ratio
M	Moisture
MS	Mass Spectrometry
PO	*Posidonia oceanica*
POW	PO waste
TANN	Tannins
TC	Total carbon
TG	Thermogravimetry
TGL	Triglycerides

(*continued on next page*)

* Corresponding author at: Department of Energy, University of Oviedo, Polytechnic School of Mieres, c/ Gonzalo Gutiérrez Quirós s/n, 33600 Mieres, Asturias, Spain.
E-mail address: riosjuan@uniovi.es (J.C. Ríos-Fernández).

https://doi.org/10.1016/j.wasman.2024.04.014
Received 6 December 2023; Received in revised form 11 March 2024; Accepted 7 April 2024
Available online 10 April 2024

Nomenclature (*continued*)

Symbols/abbreviations	
TOC	Total organic carbon
T_p	Peak temperature
VM	Volatile matter
WGSR	Water gas shift reaction

1. Introduction

Posidonia oceanica (PO) (Linnaeus) Delile, also called Mediterranean Tapeweed or Neptune Grass, is a seagrass species belonging to the family Posidoniaceae (Boudouresque et al., 1984). It is a marine plant with roots, stems, leaves, and fruits; being classified as a marine angiosperm of subtropical climate (Ruipérez et al., 2012). PO colonies constitute true seagrass meadows and are exclusive to the Mediterranean Sea, occupying an area of between 25,000 and 50,000 km^2 (Pasqualini et al., 1998), growing at all latitudes from Libya (31°0′N) to the Gulf of Trieste (45°40′N) (Green and Short, 2003). The Spanish Balearic Islands are home to the largest PO reef in the world (Aires et al., 2011), specifically, in the protected natural area of Ses Salines d'Eivissa i Formentera, between the islands of Ibiza and Formentera. The horizontal growth rate of Posidonia oceanica is 6 cm/year, while the vertical growth rate is 1 cm/year (Ruipérez et al., 2012). It has a high production rate, which has been estimated at 200 ± 300 g/m^2 per year (Cebrian and Duarte, 2001), mainly due to the annual growth of the leaves. The leaves of PO are continually renewed because it is a deciduous plant. They grow in spring, and with spring and autumn storms, they lose their oldest leaves, which turn brown and are photosynthetically inactive. It is especially in autumn when storms tear off more leaves and accumulate the fallen remains on the beaches (Ruipérez et al., 2012), forming large clumps of PO. It is estimated that 34 % of the leaves that fall off the plant wash up on beaches (Ruipérez et al., 2012), where they either decompose or are collected and treated as urban solid waste, currently without recovery. In recent years, there has been an increase in the arrival of leaves in spring due to the increase in storms before the summer season, which together with increased pressure from the tourist sector, has increased the volume of PO waste (POW) collection. In 2004, Borum et al. (2004) quantified the amount of PO litter generated per kilometre of meadow per year at 125 kg. PO litter deposited in Mediterranean coastal areas is an environmental, economic, hygienic, and social problem (Balata and Tola, 2018). It is of particular importance in the areas with the greatest tourist involvement (Cocozza et al., 2011). The annual rate of accumulation of PO necromass is estimated to be between 70 and 660 g/m^2 (Gazeau et al., 2005). Other authors have quantified this production as 300 and 2000 g/m^2 (Bay, 1984; Bianchi et al., 1989; Jiménez et al., 1996; Terrados and Duarte, 2000). For a pasture width of 1 km, the annual deposition per metre of beach is approximately 125 kg of dry matter per kilometre of seagrass meadow (Cocozza et al., 2011). Therefore, extrapolating these data to the estimated total area of PO meadows, around one million tonnes of PO necromass is generated on the Spanish coasts, mostly leaves, the decomposition of which is extremely slow (Romero, 2004). This amount will increase enormously if we consider the large coastal area where Posidonia is deposited throughout the entire Mediterranean. Disposal is usually carried out by sending POW to landfills, at a high economic cost for public administrations. It should be borne in mind that most of the areas where this marine debris is deposited are areas of great importance for tourists, making it essential to keep the beaches and coastline in perfect condition. The present study (on the pyrolytic valorisation of the residual biomass of PO leaves) agrees with the research that, in the opinion of the Spanish Ministry of the Environment and Rural and Marine Affairs, is important for making progress in the conservation of habitat type 1120 (PO meadows). Specifically, it can be classified within the field of research entitled "Possible uses of *P. oceanica* litter that is fireproof and rich in tannins and salts, and sustainable ways of exploitation" which appears in the publication "Preliminary ecological bases for the conservation of habitat types of Community interest in Spain", promoted by the Directorate General for the Natural Environment and Forestry Policy of the Ministry of the Environment and Rural and Marine Affairs of the Government of Spain. The Spanish proposal joins the rest of the strategies adopted by the members of the European Union according to the objective of the Habitats Directive (European Council, 1992) to promote the conservation status of a set of natural habitats. The valorisation of this type of biomass (POW) would avoid the economic and environmental costs derived from its disposal as waste.

Mechanical means, such as a tractor equipped with a bucket designed to minimize the extraction of sand and a truck for transport to the waste treatment plant, are used to remove the remains of PO from the beaches (Balata and Tola, 2018). The cost of this process is comparable to that of solid urban waste and varies depending on the location of the beach (BOIB, 2023). In European Mediterranean countries, the cost of waste treatment is typically around 115–150 € per ton (De Falco et al., 2008).

An option for POW management may imply a thermal valorisation, such as pyrolysis, which transforms this waste into biogas, biochar or bio-oil or produces added-value compounds. The production of biogas may be an attractive alternative, since European Biogas Association estimates that biogas and biomethane generation can be quadruple in 2050 with respect to that of 2019 (Bencoova et al., 2021).

To ensure the effectiveness of pyrolysis technologies, the raw material must be of consistent quality and quantity (Maroušek et al., 2023a). On the one hand, as was mentioned, significant quantities of PO residue reach the coasts each year (Terrados and Duarte, 2000). Although the amount may vary annually, it is still substantial enough to be used for energy purposes (Terrados and Duarte, 2000). It is worth noting that Simeone (2008) estimated the sediment concentration in PO berms to be between 47.5 and 70.0 $kg{\cdot}m^{-3}$. On the other hand, organic matter of PO leaves does not vary significantly with the time of the year or the location. Another issue is the inorganic matter of POW, whose variation should be studied thoroughly.

For a technology to be sustainable, it must first be profitable (Pavolova and Bakalár, 2021). Additionally, Maroušek et al., (2023b) have reported the current difficulty of running a profitable business for biodiesel from algae, due to the high costs associated to algae production. In the case of the energy use of POW, public administrations could save the expense caused by its elimination from beaches and generate a source of income linked to the use of this waste. The exploitation of these resources could benefit local administrations, but it could also be subject to business use by establishing public or private companies. This could be favourable for boosting the exploitation of these resources (Akbari et al., 2021).

Compared with other types of biomasses, the main limitation of POW as a potential source of energy production is its high ash yield (Neven et al., 2019). Although some articles have focused on thermal processing (pyrolysis and gasification) or co-processing and anaerobic digestion of PO for obtaining bioethanol (Pilavtepe et al., 2013), biofuel (Zaafouri et al., 2016), biochar (Moltó et al., 2022), and biogas (Maisano et al., 2019), there has been no research on the effect of POW inorganic matter on its pyrolysis.

POW contains marine salt, epiphytes, and sand. Thus, among other inorganics, it has Si, Fe and abundant alkali and alkali earth metals (AAEMs), mainly in the form of Na, Mg and K chlorides and Ca and Mg carbonates. AAEMs favour deoxygenation reactions, which produces more char and gas (the latter upgraded) and less bio-oil but with higher C/O ratio (Wang et al., 2022). AAEMs also ease the breakage of biopolymers' structure, which shifts thermal degradation to lower temperatures (Wang et al., 2022). On the other hand, CaO and CaO/Fe_2O_3 promote H_2 generation during biomass pyrolysis (Widyawati et al., 2011) and biomass steam generation (Hu et al., 2020), respectively. Moreover, calcite has been widely used in industry for capturing SO_2

during thermal processing (Dasgupta et al., 2003). After these considerations, one might ask if the pyrolysis of POW without removing its inorganic matter could be advantageous and how it affects the decomposition of POW organic macromolecules. Obviously, the lack of pretreatment would reduce complexity and costs of POW management and facilitate it, and, perhaps, it would allow us to obtain final products with better quality and/or to develop more environmentally friendly processes. Additionally, there exist numerous issues that still must be researched to understand the effect of inorganic matter on biomass pyrolysis, including AAEMs influence (Wang et al., 2022). Thus, this manuscript is focused on the study of the effect of POW natural inorganic matter (marine salt, epiphytes, and sand) on its pyrolysis. For this aim, two samples, one without pretreatment ($POW_{unwashed}$) and the other being previously washed with distilled water (POW_{washed}), were pyrolyzed, studied and compared. Thus, the decomposition of POW biopolymers, the release of several compounds and the effect of inorganic matter were addressed. This knowledge is crucial for an optimum design of POW pyrolysis depending on the objective sought.

2. Material and methods

2.1. Material and ultimate analysis

Waste of PO (POW) was collected from a beach of Ibiza Island (Spain) (at the coordinates 38°58′17.324″N, 1°17′12.116″E) in July 2021. 15 g of this raw waste (only leaves) were submerged in a container with 3.5 l of distilled water for 24 h. After this stage, the washed PO (POW_{washed}) was air dried at the ambient temperature of the laboratory and ground to a particle size lower than 250 μm.

Ultimate analysis (C, H, N and S) was carried out in a Vario Macro Elementar Analyzer, which reaches a temperature of 1150 °C. A TOC analyser (Shimadzu TOC-V CSH) was used for determining total carbon (TC), inorganic carbon (IC), and total organic carbon (TOC).

2.2. Concentrations of some major, minor and trace elements and X-ray diffraction (XRD)

The concentrations of the elements B, Na, Mg, Al, P, K, Ca Ti, V, Mn, Fe, Co, Ni, Cu, Zn, As, Se, Sr, Mo, Ag, Cd, Sn, Sb, Ba, Hg, Pb, and U in both samples were determined by using Isotope Dilution Analysis (IDA) combined with Inductively Coupled Plasma Mass Spectrometry (ICP-MS) after digestion with reverse aqua regia.

For identifying the main crystalline minerals of $POW_{unwashed}$ and POW_{washed}, their diffractograms were obtained in a PANalytical X'Pert Pro diffractometer with a Bragg-Brentano configuration and Omega-2Theta scan. Diffraction intensities were recorded using continuous sweep, with a scanning rate of 0.025°/s for a 2θ range from 5° to 80°, points were interpolated every 0.013° for 2θ and with a counting time of approximately 135 s.

2.3. Thermogravimetry (TG) and mass spectrometry coupled to TG (TG/MS)

Thermogravimetric analyses (TGA) were carried out in a thermobalance Mettler TGA/SDTA 851^e. Its exit was connected to a mass spectrometer ThermoStar Pfeiffer Vacuum by a 200 °C thermostated pipe to avoid gas condensation. In the TG runs, flow rates of both N_2 and O_2 of 50 cm^3/min were used as reaction gases. The samples were heated at a rate of 10 °C/min from ambient temperature up to 800 °C. TGs were repeated, the difference being lower than 5 wt% for every temperature. Derivative TG (DTG) curves were also obtained. The thermobalance was coupled to a Pfeiffer Vacuum ThermoStar GSD301T mass spectrometer. By a detector C-SEM, operating at 1200 V and with a time constant of 1 s, several components were identified by the mass-to-charge ratios (m/z) of key fragment ions. The fragment ions at (m/z)s 2, 12, 15, 16, 18, 25, 29, 31, 34, 38, 41, 44, 45, 46, 50, 58, 60, 64, 68, 72, 80, 94, 96, 110, 109 were assigned to H_2 (hydrogen), CO (carbon monoxide), CH_4 (methane), O (oxygen), H_2O (water), C_2H_2 (acetylene), HCHO (formaldehyde), CH_3OH (methanol), H_2S (hydrogen sulphide), HCl (hydrogen chloride), C_3H_6 (propene), CO_2 (carbon dioxide), CH_3COOH (acetic acid), HCOOH (formic acid), CH_3Cl (chloromethane), C_3H_6O (propanal), COS (carbonyl sulphide), SO_2 (sulphur dioxide), C_4H_4O (furan), Cl_2 (chlorine), H_2SO_4 (sulphuric acid), C_6H_6O (phenol), $C_5H_4O_2$ (furfural), $C_6H_6O_2$ (catechol), $C_7H_8O_2$ (guaiacol), respectively.

2.4. TGA-based proximate analysis, organic C from TGA and HHV

Proximate analysis was deduced from thermogravimetric analysis (TGA), combustion and pyrolysis profiles. Although, the values are indicative, they allow us to compare both samples ($POW_{unwashed}$ and POW_{washed}) and observe the effect of removing part of its inorganic matter.

Moisture (M) was determined as the mass loss up to 150 °C. The two ash yields at 550 °C and 800 °C (A_{550} and A_{800}, respectively) are equal to the combustion TG percentages at the above temperatures. Fixed carbon (FC) was calculated subtracting combustion TG at 800 °C (A_{800}) to the pyrolysis TG at the same temperature (CY_{800}). Accordingly, volatile matter (VM) in dry basis is equal to 100 – A_{800} – FC. The subtraction A_{550}–A_{800} gives an estimation about the quantity of CO_2 released from carbonates ($CaCO_3$ and $MgCO_3$) and, therefore, about C in the sample that is in the form of carbonates ($C_{carbonates}$). This is confirmed by the fact that only CO_2 (neither SO_2/SO_3 nor H_2O) was detected by combustion with O_2 using TG-mass spectrometry (TG/MS) analysis in this interval (550 °C–800 °C). The substraction of $C_{carbonates}$ from total C gives organic C (C_{org}). The fact that C_{org} in daf basis is nearly equal for both samples (POW_{washed} and $POW_{unwashed}$) also proves that the calculation is correct. Higher heating value (HHV) was calculated from ultimate analysis, using Yin's equation (Yin, 2011). This equation considers C and H biomass contents. Other equations that calculate HHV from C, H and O contents (Shen and Azevedo, 2005; Demirbas et al., 1997) give very similar results for this sample and they use O, which is an estimation from other element concentrations.

2.5. Structural analysis from Debiagi et al.'s characterization method (Debiagi et al., 2015)

Lignocellulosic composition was determined according to Debiagi et al.'s procedure (Debiagi et al., 2015). They proposed a characterization method for predicting structural composition, including extractives, from ultimate analysis. With this method (Debiagi et al., 2015), the components cellulose (CELL: $C_6H_{10}O_5$), hemicellulose (HCELL: $C_5H_8O_4$), three different types of lignin (LIG-C: $C_{15}H_{14}O_4$, LIG-H: $C_{22}H_{28}O_9$ and LIG-O: $C_{20}H_{22}O_{10}$), tannins (TANN: $C_{15}H_{12}O_7$) and triglycerides (TGL: $C_{57}H_{100}O_7$) can be determined. Lignin (LIG) can be considered as a weighted combination of three units, LIG-C, LIG-H and LIG-O, which have decreasing ratios of $(C/O)_{molar}$ (Debiagi et al., 2015). C_{org}, H and O contents of the samples (POW_{washed} and $POW_{unwashed}$) in daf basis and normalized to 100 can be expressed as a linear combination of the above components using the splitting parameters α/β/γ/δ/ε (Debiagi et al., 2015).

3. Results and discussion

3.1. POW characterization

Table 1 shows ultimate and estimative TGA-based proximate analysis, carbon contents (TC, IC and TOC), and HHV of the two samples of POW ($POW_{unwashed}$ and POW_{washed}). Table S1 shows the concentrations of some major, minor and trace elements in $POW_{unwashed}$ and POW_{washed}. In Fig. S1, the diffractograms of $POW_{unwashed}$ and POW_{washed} can be observed. The minerals aragonite ($CaCO_3$), dolomite ($(Mg_{0.129}Ca_{0.871})(CO_3)$), halite (NaCl), bassanite ($CaSO_4{\cdot}0.67H_2O$),

Table 1
POW ultimate, TOC and TGA-based proximate analyses.

	$POW_{unwashed}$	POW_{washed}		$POW_{unwashed}$	POW_{washed}
TGA-based proximate analysis					
Moisture (wt% ad)	9.6	13.1			
Volatile matter (wt% db)	56.6	67.3			
Fixed carbon [a] (wt% db)	6.6	16.7			
Ash at 550 °C (wt% db)	50.7	24.3			
Ash at 800 °C (wt% db)	36.7	16.0			
Ultimate analysis					
C (wt% db)	27.36	38.40	C (wt % daf)	55.45	50.66
H (wt% db)	2.89	4.29	H (wt % daf)	8.26	7.90
N (wt% db)	0.48	0.64	N (wt % daf)	0.97	0.85
S (wt% db)	2.10	0.95	S (wt % daf)	4.25	1.25
O[a] (wt% db)	30.44	39.72	O[a] (wt% daf)	31.07	39.34
C from carbonates[b]					
$C_{carbonates}$ (wt% db)	3.8	2.3			
Organic C[a]					
C_{org} (wt% db)	23.6	36.1	C_{org} (wt% daf)	47.9	47.7
Carbon from TOC analysis					
TC (wt% db)	27.13	38.77			
IC (wt% db)	4.13	2.46			
TOC (wt% db)	23.01	36.31			
Higher heating value (MJ/kg)	10.4	14.9			

daf basis was calculated using ashes at 550 °C.
[a] Calculated by difference.
[b] Calculated from TGA.

akaganeite ($Fe_{+3}O(OH)$), gypsum ($CaSO_4(H_2O)_2$) and quartz (SiO_2).

The comparison of the TGA-based proximate analysis shows that POW washing reduced inorganic matter (SiO_2, carbonates, chlorides, sulphates, etc.) substantially. This is confirmed by ICP analysis (Table S1) and DRX (Fig. S1), since there is a significant loss of some element (Na, Mg, Al, K, Ca, Fe, Sr) content due to the washing, especially the alkali and alkali earth metals of this group. Additionally, halite and bassanite disappear in POW_{washed} (Fig. S1).

However, A_{800} and A_{550} values are still high in POW_{washed} (16.0 wt% db and 24.3 wt% db, respectively). The subtraction of these values is approximately equal to the CO_2 released from carbonates (from 550 °C to 800 °C). Thus, it allows us to estimate the remaining carbonates (mainly associated to epiphytes) expressed in $CaCO_3$ equivalent, which gives 19 wt% (db). Comparing POW_{washed} and $POW_{unwashed}$, around 40 % of carbonates have been removed. These calculations are confirmed by the results of TOC analysis (Table 1). Epiphytes are small calcareous organisms located on the surface of PO leaves that shed from POW during the washing. Coralline algae epiphytes, typical of PO (Gambi et al., 2010), incorporate aragonite and dolomite into their tissues or structures for support and protection (Nash et al., 2013).

Ultimate analysis of $POW_{unwashed}$ (Table 1) shows relatively similar values to the mean reported by other researchers (Neven et al., 2019). The most noticeable differences are in H, N and S contents, S being higher (2.10 wt% db vs. 1.87 wt% db) and H and N being lower (2.89 wt % db vs. 3.81 wt% db and 0.48 wt% db vs. 1.78 wt% db, respectively) in $POW_{unwashed}$.

Due to the differences in moisture contents and ash yields, for an adequate comparison of $POW_{unwashed}$ and POW_{washed}, ultimate analysis must be expressed in dry ash free (daf) basis (Table 1). As can be seen in Table 1, both analyses are quite similar. S content shows the highest difference, being significantly reduced by POW washing. It is due to the removal of the sulphates of POW, since bassanite disappears with washing and gypsum diminishes (Fig. S1). This agrees with the fact that sulphates and chlorides are highly mobile during biomass treatment with solvents (Vassilev et al., 2012).

In POW_{washed}, C and H contents in daf basis are slightly lower than those in $POW_{unwashed}$, due to the removal of carbonates and, probably, hydroxides. Due to the washing, a decrease of akaganeite is observed in Fig. S1. Thus, TGA-based proximate and ultimate analyses seem to indicate that mainly inorganic matter is lost in POW washing with distilled water.

HHV of $POW_{unwashed}$ (10.4 MJ/kg) is like the one reported by Neven et al. (Neven et al., 2019) (10.04 MJ/kg).

Table 2 shows the lignocellulosic composition of POW, as well as tannins and triglycerides, calculated according to Debiagi et al's method (Debiagi et al., 2015). The results show that the concentration of lignin in $POW_{unwashed}$ is lower than data reported by other researchers (Khiari et al., 2010; Neven et al., 2019) and, consequently, the opposite occurs with hemicellulose content.

However, POW structural composition can vary substantially depending on the degree of material degradation and what parts of PO are in the waste. While Khiari et al. (2010) used POW balls in their research, the sample of this work only contains leaves, without sheaths. Leaf sheaths of PO are especially rich in lignin (Kaal et al., 2018).

On the other hand, due to washing with distilled water, in addition to mineral matter, mainly lignin (LIG-C and specially LIG-H) and

Table 2
POW lignocellulosic composition from Debiagi et al.'s method (Debiagi et al., 2015).

	$POW_{unwashed}$	POW_{washed}
Structural analysis (wt% daf)		
α/β/γ/δ/ε	0.6/0.8/1/0.7/0.7	0.6/0.8/1/0.7/0.7
CELL	40.4	42.4
HCELL	26.9	28.3
LIG-C	2.3	0.21
LIG-H	9.3	0.84
LIG-O	11.2	19.5
LIG	22.9	20.5
TANN	4.8	8.3
TGL	5.0	0.45
CELL, HCELL and LIG normalized to 100 (wt% daf)		
CELL (wt% daf)	47.1	46.5
HCELL (wt% daf)	29.8	31.0
LIG (wt% daf)	25.4	22.5
Extractives (wt% db)		
TANN	2.4	7.0
TGL	2.5	0.38

triglycerides (TGLs) have been removed (Table 2). Once the external protective layer (cuticle) has started to degrade, in distilled water, certain hydration had probably occurred, which led to the oxidation and breakage of structures. The fact that POW_{washed} lignin is enriched in LIG-O in comparison with $POW_{unwashed}$ indicates a higher degree of oxidation, since LIG-O is the type of lignin with higher $(O/C)_{molar}$ ratio.

3.2. POW_{washed} pyrolysis profile

The pyrolysis profile of POW_{washed} shows a significant loss of water (13.1 wt% ad) below 150 °C (Fig. S2). Between 150 °C and 210 °C, there exists a small peak that can be attributed to some extractive degradation (Sebio-Puñal et al., 2012; Folgueras et al., 2023). Between 210 °C and 360 °C, a main peak with a shoulder at the left side can be seen. In the interval 210 °C–300 °C (shoulder), the mass loss (12.4 wt% ad) is mainly due to hemicellulose decomposition, although some extractives and lignin (especially those more thermally unstable LIG-O and LIG-H) contribute in lower proportion. Only when lignin starts its degradation, hemicellulose and cellulose also begin their thermal decomposition (Folgueras et al., 2023), since lignin acts as a "reinforcing mesh" (Wang et al., 2017) avoiding carbohydrate decomposition. In the range 300 °C–360 °C, the main peak occurs (329 °C), which is related to cellulose decomposition and, to a lesser extent, to hemicellulose and lignin thermal degradation. From 360 °C, POW decomposition is mainly associated with lignin pyrolysis, a small peak at around 470 °C occurring. At temperatures higher than 200 °C, lignin pyrolysis is probably a melt radical process, where several reactions compete (Faravelli et al., 2010). On the other hand, probably at 360 °C, there exists a solid product (char) that undergoes further polymerization through the reaction of radicals (aromatics, alkanes and alkenes) (Chu et al., 2013). This char is transformed into a polyaromatic char after the loss of hydroxyl and methoxy groups (Chu et al., 2013).

Finally, the peak with a maximum at 741 °C is due to carbonate decomposition. Aragonite and dolomite were found in POW_{washed} (Fig. S1).

3.3. Comparison of POW_{washed} and $POW_{unwashed}$ pyrolysis

Fig. 1 shows pyrolysis DTGs of POW_{washed} and $POW_{unwashed}$ in daf basis (A_{550}) from 150 °C to 550 °C. The volatile matter released in this interval is around 70 wt% (daf) in both samples, being 70.1 and 71.6 wt % (daf) for POW_{washed} and $POW_{unwashed}$, respectively.

This means that washing does not substantially affect the total volatile matter released between 150 °C and 550 °C, although the way it is emitted changes.

As can be seen in Fig. 1, for the unwashed sample, hemicellulose pyrolysis in the range 210 °C–300 °C is accelerated, the maximum rate of its peak being reached at 275 °C, approximately 35 °C before than of POW_{washed}. Therefore, for $POW_{unwashed}$, there is a lower degree of overlapping between hemicellulose and cellulose pyrolysis, because hemicellulose degradation occurs more quickly at lower temperatures. The mass loss weights in the range 210 °C–300 °C are 18.9 and 23.1 wt% (daf) for POW_{washed} and $POW_{unwashed}$, respectively. For $POW_{unwashed}$, 23.1 wt% (daf) is like hemicellulose content in daf basis 26.9 wt% (daf) (Table 2), which seems to indicate that the structural composition estimation via Faravelli et al's method is quite accurate. The acceleration in hemicellulose pyrolysis may be because $POW_{unwashed}$ contains more alkali and alkaline earth metals (Table S1) that act as catalysers (Fahmi et al., 2007; Wang et al., 2022). Moreover, this agrees with the fact that hemicellulose is the structural component of biomass that contains more inorganics (Cagnon et al., 2009), being richer in sulphates, chlorides, nitrates and silicic acid (Vassilev et al., 2012). This may indicate that, in $POW_{unwashed}$, there is a quicker breakage of β-O-4 structures in lignin and hydrogen bonds in hemicellulose. This breakage could be accelerated by the presence of alkali metal salts, such as K salts (KOH, K_2CO_3) and/or Na salts (NaOH and Na_2CO_3), etc., which can act as oxygen carriers (Boxiong and Qinlei, 2006). On the other hand, Fe_2O_3 may intervene in the quick decomposition of hemicellulose in $POW_{unwashed}$, since Fe_2O_3 can also be another oxygen carrier that weakens C—C and C—H bonds, avoiding the formation of stable chemical compounds (Iáñez-Rodríguez et al., 2019). During heating, akaganeite (Fig. S1) is transformed into Fe_2O_3 (Peterson et al., 2018).

In contrast, cellulose pyrolysis seems not to be significantly affected by the washing of POW.

Fig. 2 shows "$TG_{pyrolysis}$ – $TG_{combustion}$" in daf basis (A_{550}) versus temperature in the range 550 °C–800 °C for both samples. Assuming that during combustion with O_2, at 550 °C, nearly all the organic matter has been removed, "$TG_{pyrolysis}$ – $TG_{combustion}$" estimates the rate of decomposition of the remaining organic matter (char) during POW pyrolysis at each temperature "t". As was previously mentioned, at 550 °C, the remaining organic matter (char) is around 30 wt% (daf) (Fig. 2).

"$TG_{pyrolysis}$ – $TG_{combustion}$" is an estimation since inorganic matter transformation is not identical during pyrolysis to during combustion. Additionally, $POW_{unwashed}$ contains more inorganic matter, which influences organic matter pyrolysis. Despite these factors, Fig. 2 can give valuable information for comparing the behaviour of the char of both samples during pyrolysis.

In the interval 550 °C–650 °C of POW pyrolysis, char evolves in the same way for both samples (Fig. 2), which reflects the interest of this comparison. Therefore, in this range, the excess of inorganic matter in $POW_{unwashed}$ seems not to affect POW organic matter decomposition substantially. The organic matter loss is around 2 wt% (daf) for both samples. Nevertheless, from 710 °C, and especially between 710 °C and 760 °C, the inorganic matter of $POW_{unwashed}$ produces a notable char decomposition. Thus, mass loss is around 8.6 wt% (daf) and 2.4 wt%

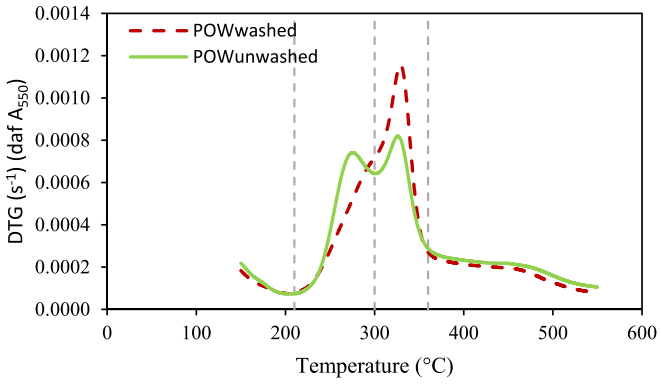

Fig. 1. Pyrolysis profiles in daf basis (A550) from 150 °C to 550 °C of POW_{washed} and $POW_{unwashed}$.

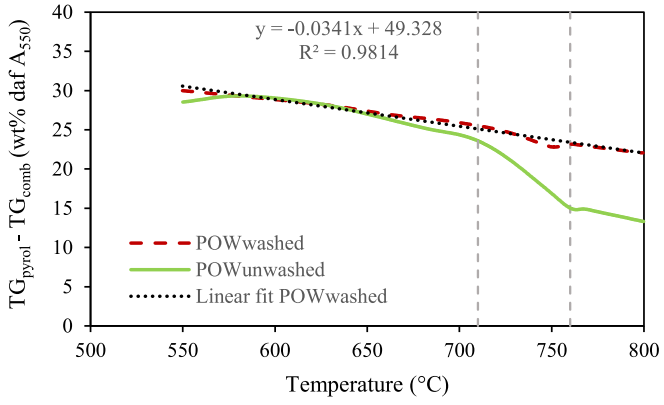

Fig. 2. Estimation of char mass loss in daf basis (A_{550}) between 500 °C and 800 °C for POW_{washed} and $POW_{unwashed}$.

(daf) for $POW_{unwashed}$ and POW_{washed}, respectively. This is probably related to the fact that there is a massive carbonate decomposition that produces char gasification (see Section 3.4.4). Thus, the high quantity of carbonates in $POW_{unwashed}$ affects char pyrolysis especially in the range 710 °C–760 °C. For POW_{washed} between 550 °C and 800 °C, the rate of char decomposition (daf basis) is roughly constant (Fig. 2).

3.4. Pyrolysis products of $POW_{unwashed}$ and POW_{washed}

For $POW_{unwashed}$ and POW_{washed} pyrolysis, Figs. 3–5 show the evolution of the studied fragment ions with temperature. On the left vertical axes of Figs. 3–5, ion intensities normalized to sample weight in daf basis (considering ashes at 800 °C) (I) are shown, while the right vertical axis show mass loss rate (DTG) in s^{-1} in daf basis (A_{800}).

The ion at *m/z* 16 is probably associated with atomic oxygen (radical O) (Fig. 3).

Although CH_4, CH_3Cl and NH_3 may also contribute to this *m/z*, it does not evolve similarly to other (*m/z*)s of these compounds. Accordingly, hydrocarbon flame gases, a considerable quantity of atomic oxygen can be present (David et al., 1948).

Pyrolysis can be divided, at least, into primary and secondary stages. During primary pyrolysis, gases, tar and solid char are produced due to the heating of the sample. On the other hand, during secondary pyrolysis, reactions between compounds, cracking and reforming of gases and tar/char gasification occurs.

In general, light oxygenated compounds come mainly from carbohydrate thermal degradation, whereas aromatics and phenols and their alkyl-substituted fractions are formed from lignin (Mendu et al., 2011). This is more applicable in the first stages of pyrolysis when mainly primary products are formed. At temperatures higher than 550 °C, due to the loss of most volatiles, secondary pyrolysis becomes more relevant.

With regard to the compounds phenol (C_6H_6O), guaiacol ($C_7H_8O_2$) and catechol ($C_6H_6O_2$), phenol and guaiacol are lignin-derived compounds that come from H-units and G-units of lignin respectively (Kim et al., 2011), while catechol ($C_6H_6O_2$) is a tannin-derived compound (Kaal et al., 2018).

Due to the high concentration of NaCl in the samples (especially in $POW_{unwashed}$) (Table S1 and Fig. S1), the formation of HCl should be expected. Several studies of biomass pyrolysis have detected HCl and CH_3Cl in the emitted gases (Rahim et al., 2013; Saleh et al., 2014; Chen et al., 2016; Peng et al., 2019). However, it varies greatly depending on the type of biomass (Peng et al., 2019).

Thus, the following reactions that produce HCl may occur:

$$2\ NaCl + SO_2 + O + H_2O \rightarrow Na_2SO_4 + 2\ HCl \quad (1)$$

$$NaCl + H_2O \rightarrow NaOH + HCl \quad (2)$$

Nevertheless, HCl was scarcely detected (Fig. 4).

3.4.1. Temperature interval 200 °C–260 °C (ΔT_1)

As can be seen in Figs. 4 and 5, for POW_{washed}, several compounds (CH_4, CH_3OH, C_2H_2, C_3H_6, H_2, C_3H_6O, C_4H_4O, HCHO, $C_5H_4O_2$, C_6H_6O, $C_6H_6O_2$, CH_3Cl) show two small peaks with peak temperatures (T_p) at approximately 220 °C and 250 °C. Also, in this interval, the formation of CO, CO_2, H_2O and O begins (Figs. 3 and 4), mainly as a consequence of primary pyrolysis of lignin, hemicellulose and extractives.

The formation of phenol evinces lignin decomposition, which reveals

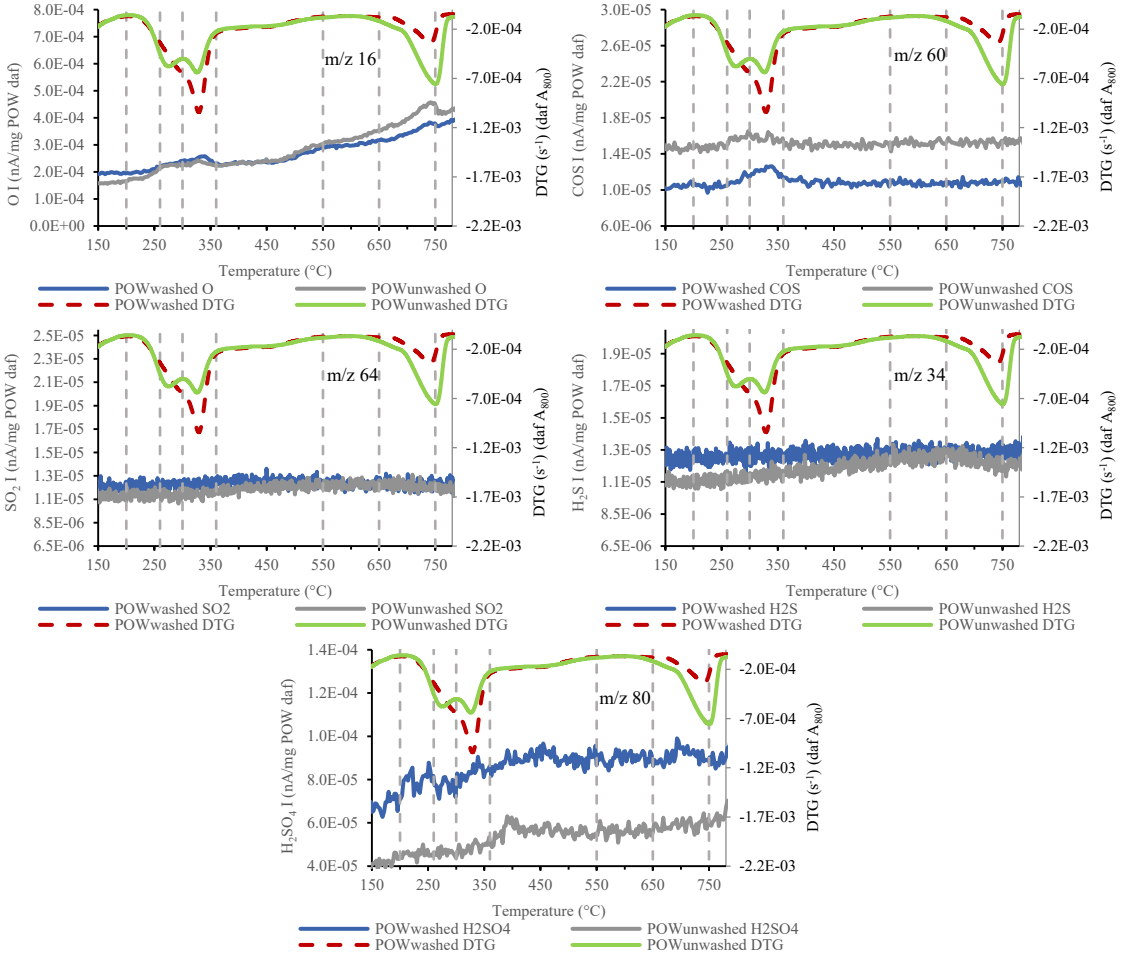

Fig. 3. Intensities (I) of oxygen (O), carbonyl sulphide (COS), sulphur dioxide (SO_2), furan (C_4H_4O), hydrogen sulphide (H_2S), sulphuric acid (H_2SO_4).

Fig. 4. Intensities (I) of carbon monoxide (CO), carbon dioxide (CO_2), hydrogen (H_2), water (H_2O), acetylene (C_2H_2), propene (C_3H_6), methane (CH_4), chloromethane (CH_3Cl), hydrogen chloride (HCl) and chlorine (Cl_2) during POW_{washed} and $POW_{unwashed}$ pyrolysis.

that β-O-4 structures breakage occurs before 200 °C. This cleavage establishes the beginning of lignin degradation by radical reactions. The release of furfural, furan and propanal, which are predominantly carbohydrate-derived compounds, indicates that hemicellulose also decomposes and probably cellulose begins its decomposition. Alkali earth metals act as catalysers, which produces furfural from the decomposition of hemicellulose at an early stage of pyrolysis (Li et al., 2020). Ca, Mg and Sr concentrations are around 13.0, 1.8 and 0.2 wt%

Fig. 5. Intensities (I) of formaldehyde (HCOH), propanal (C_3H_6O), furfural ($C_5H_4O_2$), furan (C_4H_4O), methanol (CH_3OH), phenol (C_6H_6O), catechol ($C_6H_6O_2$), guaiacol ($C_7H_8O_2$), formic acid (HCOOH) and acetic acid (CH_3COOH) during POW_{washed} and $POW_{unwashed}$ pyrolysis.

(db) for $POW_{unwashed}$ and 6.5, 0.7 and 0.08 wt% (db) for POW_{washed}, respectively (Table S1). Between 210 °C and 260 °C, pyrolysis of extractives continues, since a small amount of catechol was detected (Fig. 5).

Table 3 shows the possible reactions and/or transformations that produce H_2, O, CH_4, C_2H_2, C_3H_6 CH_3OH and CH_3Cl.

The breakage of methyl radicals from methoxy groups releases O, which would explain the formation of atomic oxygen (O) (Table 3). In

Table 3
Transformations and/or reactions (with their numbers) that produces several identified compounds between 200 and 260 °C (ΔT_1).

Compound/ element	Transformations, reactions	Reaction n°	Catalyst
H_2	Paraffins dehydrogenation (Kraiem et al., 2017)Steam reforming of hydrocarbons and/or oxygenated compounds (Widyawati et al., 2011): $C_nH_mO_p + (2n\text{-}p)\ H_2O \rightarrow n\ CO_2 + (1/2m + 2n - p)\ H_2$	(3)	
O	Breakage of methyl radicals from methoxy groups		
CH_4	Cleavage of methyl groups (CH_3·)		
C_2H_2, C_3H_6	Triglyceride decomposition (Kraiem et al., 2017)		Fe (Table S1)
	Fischer-Tropsch's synthesis (Fahim et al., 2010; Otun et al., 2020):	(4)	
	$2\ CO + 3\ H_2 \rightarrow C_2H_2 + 2\ H_2O$	(5)	
	$3\ CO + 6\ H_2 \rightarrow C_3H_6 + 3\ H_2O$		
CH_3OH	Breakage of methoxy groups (CH_3O·) (Biagini et al., 2006)		
	Recombination reaction of CH_3· with hydroxyl radical (HO·) (Hough et al., 2016): $CH_3\cdot + \cdot OH \rightarrow CH_3OH$	(6)	
CH_3Cl	$CH_4 + Cl_2 \rightarrow CH_3Cl + HCl$ (Kwon et al., 2020)	(7)	

the lignin structure, the energy of the bond (CH_3-O·) is only slightly higher than that of β-O-4 structure (Faravelli et al., 2010). Alkali metals and, especially NaOH, favour deoxygenation of methoxy groups (Wang et al., 2022). Other researchers (Li et al., 2020) also found that alkali metals promote ether bond cleavage in lignin. There exist significant concentrations of Na in the samples, which are 5.1 and 0.7 wt% in $POW_{unwashed}$ and POW_{washed}, respectively (Table S1).

The above two peaks that appear in some compound evolution of POW_{washed} are not observed in $POW_{unwashed}$ (Figs. 3–5). This could be related to the fact that POW_{washed} is enriched in TANN, LIG-O, HCELL and CELL (Table 2), reason why the above small peaks (associated to lignin, extractives, hemicellulose and to a lesser extent to cellulose decomposition) appear clearly in various compounds released by this sample. LIG-O is the structure with higher $(O/C)_{molar}$ ratio (more oxidized and less evolved) of lignin and, consequently, the one easier to degrade.

3.4.2. Temperature interval 260 °C–60 °C (ΔT_2 and ΔT_3)

In the temperature range 260 °C360 °C, from 260 °C to 300 °C (ΔT_2), mainly hemicellulose decomposes, while from 300 °C to 360 °C (end of the main DTG peak) (ΔT_3), the process is dominated by cellulose decomposition. Despite this, hemicellulose, cellulose and lignin undergo transformations in the whole interval. During primary pyrolysis of cellulose and hemicellulose, the chemical compounds formed come from two competitive pathways: i) depolymerization and ii) fragmentation (Usino et al., 2020). However, for hemicellulose, the predominant pathway is depolymerization, ring scission, and rearrangement reactions (Usino et al., 2020). On the other hand, alkali metals promote fragmentation reactions against depolymerization ones (Di Blasi, 2008; Anca-Couce, 2016). This probably occurs with $POW_{unwashed}$ and POW_{washed}, due to their high alkali metal concentrations (Table S1).

The compounds CO_2, H_2O, CO, CH_4, HCOOH and furfural and radical O are released from 260 °C to 360 °C, their evolution with temperature being like that of their corresponding DTG (Figs. 4 and 5). This similarity seems to indicate that these compounds came from both hemicellulose and cellulose pyrolysis. CO_2 was probably formed by decarboxylation of side chains of cellulose and hemicellulose (primary pyrolysis), while CO was produced by the decarbonylation reactions of unstable intermediate products (secondary pyrolysis) (Wang et al., 2013).

Furfural is one of the most important compounds derived from holocellulose pyrolysis (Hu et al., 2018) and is probably formed by depolymerization, dehydration and rearrangement from hemicellulose and cellulose (Usino et al., 2020), while formic acid may come from their side chain fragmentation (Wang et al., 2013).

One way water is formed may be:

$$H\cdot + \cdot OH \rightarrow H_2O \quad (8)$$

This agrees with other researchers' (Chu et al., 2013) observation during lignin pyrolysis, which found that water production in the range 350 °C–400 °C corresponded with the diminishing of —OH peak in char.

CH_3OH shows two significant peaks in this temperature interval (Fig. 5). The one associated with hemicellulose (ΔT_2) being higher than that of cellulose (ΔT_3). This can be related to a higher decomposition of LIG-H (more methoxy groups than LIG-O and LIG-C) during ΔT_2 and the breakage of its methoxy groups.

Other compounds that show a peak (without a clear difference between hemicellulose and cellulose) in this temperature interval are CH_3COOH, C_2H_2, C_3H_6, CH_3Cl, COS, guaiacol, catechol, H_2SO_4, formaldehyde, propanal and HCl (Figs. 3–5). The last two of these with very small peaks. Most of these compound' peaks are very small or even non-existent for $POW_{unwashed}$ (Figs. 3–5).

Table 4 shows the possible reactions and/or pathways for H_2, COS, HCHO, CH_3COOH and H_2SO_4 formation.

The formation of HCOOH through the intermediate HCOONa (Table 4) (commercially used (Hietala et al., 2016)) would explain the higher HCOOH release for $POW_{unwashed}$, since $POW_{unwashed}$ has much higher Na content (Table S1 and Fig. S1). Additionally, other researchers (Li et al., 2020) have pointed out that alkali metals promote ring-scission of sugar units, which increases acid production. Thus, through the generation of H_2SO_4, O could be related to HCOOH high intensities in $POW_{unwashed}$.

The presence of guaiacol, catechol and propanal are indicative of the decomposition of lignin (G-units), tannins and carbohydrates, respectively.

3.4.3. Temperature interval 360 °C–550 °C (ΔT_4)

In this interval of temperature, the structural component that mainly decomposes is lignin. As $POW_{unwashed}$ is enriched in LIG-H and LIG-C (Table 2) due to the washing, in this stage, certain acceleration in its pyrolysis in comparison with POW_{washed} can be observed (Fig. 1). $POW_{unwashed}$ shows a small peak at 400 °C for several compounds such as formaldehyde, H_2, CH_3OH, CO, HCOOH, C_2H_2 and C_3H_6 (Figs. 4 and 5).

Table 4
Transformations and/or reactions (with their numbers) that produces several identified compounds between 260 and 360 °C (ΔT_2 and ΔT_3).

Compound	Transformations, reactions	Reaction n°	Catalyst
H_2, COS	$CO_2 + H_2S \rightarrow COS + H_2O$	(9)	
	$CH_4 + SO_2 \rightarrow COS + H_2O + H_2$	(10)	
HCHO	$CH_3OH + O \rightarrow HCHO + H_2O$	(11)	
H_2SO_4	$H_2O + SO_2 + O \rightarrow H_2SO_4$	(12)	
HCOOH	Formation of HCOOH through the intermediate methyl formate ($HCOOCH_3$):	(13)	CH_3ONa (Rong et al., 2018)
	$CH_3OH + CO \rightarrow HCOOCH_3$	(14)	
	$HCOOCH_3 + 2H_2O \rightarrow 2HCOOH + 2H_2$		
	Formation of HCOOH through the intermediate HCOONa:	(15)	
	$CO + NaOH \rightarrow HCOONa$	(16)	
	$2\ HCOONa + H_2SO_4 \rightarrow 2\ HCOOH + Na_2SO_4$		
CH_3COOH	Breakage of O-acetyl groups of hemicellulose (primary pyrolysis) (Usino et al., 2020):	(17)	
	$CH_3OH + CO \rightarrow CH_3COOH$		

Table 5 shows some possible transformations and/or reactions that lead to the formation of H_2, HCHO, C_2H_2, CH_3COH, H_2O, CO and CH_4.

3.4.4. Temperature interval 550–750 °C (ΔT_5 and ΔT_6)

Table 6 shows the main reactions that occurs during POW pyrolysis in the temperature range 550–750 °C.

In this temperature interval, carbonate ($CaCO_3$, $Mg_{0.129}Ca_{0.871}CO_3$) decomposition (reactions 22 and 23) have a notable influence on POW pyrolysis.

The formation of CaO and MgO (reactions 22 and 23), as well as Fe_2O_3 formed from akaganeite heating, can react with HCl or NaCl to form chlorides (reactions 24 and 27) and with SO_2 and O to form sulphates (reactions 28 and 29).

As there are notable amounts of carbonates in the samples (Fig. S1), reactions 24, 25, 28 and 29 can be responsible for the capture of the majority of HCl and SO_2 formed, which would explain the fact that hardly any HCl and SO_2 emissions were observed in POW pyrolysis (Figs. 3 and 4).

From 550 °C to 650 °C (ΔT_5), significant production of H_2, especially in POW_{washed}, is observed (Fig. 4), which can be attributed to partial oxidation of CH_4 (reaction 30) and steam and CO_2 reforming of CH_4 (reactions 31 and 32) and oxygenated compounds (reaction 3), such as HCOOH, with water formed in reactions 24–26.

However, H_2 production is accompanied not only by CH_4 decrease, but also by that of CO_2 from 500 °C to 600 °C (Fig. 4). Apart from reaction 32, this fact can be related to water gas shift reaction (WGSR) since the formation of H_2 and CO_2 from decarbonation reverses reaction 33.

Inherent alkali metals and alkaline earth metals (AAEMs) in biomass pyrolysis at temperatures between 500 °C and 900 °C favours H_2 production reactions, WGSR, reforming reactions and tar cracking (Hu et al., 2015). However, these effects depend greatly on AAEMs concentration and on the presence of other compounds.

As was mentioned, from 550 °C to 650 °C (ΔT_5), the loss of organic matter (char) is low and approximately equal for both samples (Fig. 2), which agrees with the fact that H_2 may come from secondary pyrolysis (reactions 31, 3 and 33). Additionally, the quantity of carbonates in the samples does not play a role as relevant as it does at higher temperatures, since decarbonation is not so intense at these temperatures.

At temperatures higher than 650 °C (Fig. 4), the formation of CO_2 from reactions 22 and 23 is very significant, especially in $POW_{unwashed}$. Thus, in this sample and due to the reversal of reaction 33, CO_2 intensity in $POW_{unwashed}$ is lower than in POW_{washed}, while that of CO is higher.

In the interval ΔT_5, some CaO and Fe_2O_3 still present in the samples can act as oxygen carriers favouring H_2 formation. Fe_2O_3/CaO mixtures promote H_2 generation during steam gasification (Hu et al., 2020). On the other hand, Fe_2O_3 may be reduced into Fe/FeO with reducing gases (CO, etc.) formed during pyrolysis (Hu et al., 2020), which may release O (it increases significantly during ΔT_5 and ΔT_6 especially in $POW_{unwashed}$). Later, reduced forms of Fe can be re-oxidized with steam into other species such as $Ca_2Fe_2O_5$ (reaction 34) (Hu et al., 2020).

Thus, H_2 may be produced by: (i) steam reforming of volatile compounds; (ii) re-oxidation of reduced iron; (iii) WGSR, and (iv) tar cracking (Widyawati et al., 2011; Hu et al., 2020). Additionally, the role of CaO is complex, since it acts as an absorbent, reactant, and catalyst in tar cracking reactions (Chen et al., 2017). They suggested that, during biomass pyrolysis at temperatures higher than 600 °C, its role as a catalyst becomes more relevant (Chen et al., 2017).

In the interval 650–750 °C (ΔT_6) of POW pyrolysis, there is a significant production of CO_2, CO and HCOOH (Figs. 4 and 5). The explanation may be related mainly to carbonate decomposition and char gasification.

Atomic oxygen and CO_2, as well as the steam formed in reactions 24–26, can act as gasifying agents of POW char, according to the reactions 35–39.

Reactions 35, 37 and 39 would explain the high intensity of CO in this interval, although the reversal of reaction 33 may also play a significant role. Some researchers (Shoja et al., 2013) highlighted the importance of reaction 39 (Boudouard) during the last stage of pyrolysis. Reaction 40 also occurs.

Both Fig. 2 and Fig. 4 for CO show that, from approximately 700 °C, the rate of char weight loss for $POW_{unwashed}$ changes with respect to POW_{washed}, evolving much more quickly for $POW_{unwashed}$. Thus, the higher carbonate content of $POW_{unwashed}$ (Fig. S1) may be responsible for the greater char loss (gasification) in this sample due mainly to reactions 22, 24, 37 and 38.

H_2 can also act as a gasification agent producing CH_4 (reaction 41),

Table 6
Reactions during POW pyrolysis between 550 and 750 °C (ΔT_5 and ΔT_6).

Process	Equations	Reaction n°
Decarbonation: $CaCO_3$, $Mg_{0.129}Ca_{0.871}CO_3$	$CaCO_3 \rightarrow CaO + CO_2$ (≥550 °C) (Bazargan et al., 2015)	(22)
	$Mg_{0.129}Ca_{0.871}CO_3 \rightarrow 0.129\ MgO + 0.871\ CaO + CO_2$ (≥500 °C)	(23)
Chlorides ($CaCl_2$, $MgCl_2$ and $FeCl_3$) formation	$CaO + 2\ HCl \rightarrow CaCl_2 + H_2O$ (Vassilev et al., 2013)	(24)
	$MgO + 2\ HCl \rightarrow MgCl_2 + H_2O$ (Vassilev et al., 2013)	(25)
	$Fe_2O_3 + 6\ HCl \rightarrow 2\ FeCl_3 + 3\ H_2O$ (Vassilev et al., 2013)	(26)
	$Fe_2O_3 + 6\ NaCl \rightarrow 2\ FeCl_3 + 3\ Na_2O$ (Vassilev et al., 2013)	(27)
Sulphation: CaO, MgO	$CaO + SO_2 + O \rightarrow CaSO_4$	(28)
	$MgO + SO_2 + O \rightarrow MgSO_4$	(29)
Partial oxidation: CH_4	$CH_4 + O \rightarrow CO + 2\ H_2$	(30)
Steam and CO_2 reforming: CH_4	$CH_4 + H_2O \rightleftharpoons CO + 3\ H_2$	(31)
	$CH_4 + CO_2 \rightleftharpoons 2\ CO + 2\ H_2$	(32)
Water gas shift reaction (WGSR)	$CO + H_2O \rightleftharpoons CO_2 + H_2$	(33)
Ca ferrite ($Ca_2Fe_2O_5$) formation	$2\ CaO + 2\ Fe + 3\ H_2O \rightarrow Ca_2Fe_2O_5 + 3\ H_2$ (Hu et al., 2020)	(34)
Gasification of char	$C + O \rightarrow CO$	(35)
	$C + 2O \rightarrow CO_2$	(36)
	$C + H_2O \rightarrow CO + H_2$	(37)
	$C + H_2O \rightarrow CO_2 + 2H_2$	(38)
	$C + CO_2 \rightarrow 2\ CO$	(39)
CO oxidation	$CO + O \rightarrow CO_2$	(40)
Methanation	$C + 2\ H_2 \rightarrow CH_4$	(41)

Table 5
Transformations and/or reactions (with their numbers) that produces several identified compounds between 360 and 550 °C (ΔT_4).

Compound	Transformations, reactions	Reaction n°	Catalyst
H_2, HCHO	Methanol dehydrogenation:		At 400 °C, synthetic mica ($NaMg_{2.5}(Si_4O_{10})F_2$) (Usachev et al., 2004)
	$CH_3OH \rightarrow HCHO + H_2$	(18)	
C_2H_2, CH_3COH (acetaldehyde)	Ethanol (CH_3CH_2OH) dehydrogenation (Idriss and Seebauer, 2000)		CaO, Fe_2O_3, SiO_2
H_2O, CO	Formic acid decarbonylation:		H_2SO_4 (Li et al., 2008)
	$HCOOH \rightarrow CO + H_2O$	(19)	
CH_4	Hydrocracking of C_2H_2 and C_3H_6:		
	$C_2H_2 + 3\ H_2 \rightarrow 2\ CH_4$	(20)	
	$C_3H_6 + 3\ H_2 \rightarrow 3\ CH_4$	(21)	

which would explain certain production of this compound at high temperatures and the decreasing of H_2 after 600 °C (Fig. 4).

Other researchers (Widyawati et al., 2011) also found that CaO promotes the formation of H_2 through reforming and char gasification reactions.

The significant production of HCOOH at these temperatures can be attributed to the high quantities of CO release (from char gasification) and the existence of NaOH, according to reactions 15 and 16.

As was discussed, by sulphate and H_2SO_4 formation, the release of atomic oxygen may be involved in the retention of SO_2 and the high intensities of HCOOH (i.e., organic compound with high oxidation state of carbon).

3.5. Some final considerations

This research does not try to define a specific procedure for valorising POW by pyrolysis, but it deepens on how POW pyrolysis occurs and how detrital inorganic matter left in the sample can affect the process. This knowledge can help to decide what should be done with POW natural inorganic matter prior to its pyrolysis, depending on the objective sought. If biogas production is required, the presence of certain inorganic matter may be interesting, since SO_2 and HCl release is negligible. However, if bio-oil is sought, the presence of marine salt and epiphytes in POW can increase the concentration of HCOOH in it. On the other hand, although the increase of salts and other inorganics in POW, may worsen pyrolysis energy balance, the existence of $CaCl_2$ (reaction 24) and $FeCl_3$ (reactions 26 and 27) in the char could produce a phosphorus-enriched biochar that has very interesting applications as a cement substitute (Maroušek et al., 2023c). A different issue would be the production of HCOOH or other value-added compounds or the recovery of part of its nutrients. Some studies have pointed out the importance of recovering nutrients from biowastes and its economic feasibility (Maroušek and Gavurová, 2022; Stávková and Maroušek, 2021).

Additionally, POW composition, especially its inorganics, can vary greatly depending on its origin and time of year. Thus, pretreatment of POW, has to be designed for every case, according to the characteristics and composition of feedstock and the pursued objectives. Scientific literature shows several examples of optimized pretreatment designs, such as the use of pressure shockwaves alone or combined with enzymatic hydrolysis (Maroušek, 2013a; Maroušek et al., 2013b) that can be considered and studied.

Obviously, for a commercial application, further research is needed to optimize POW pyrolysis conditions according to feedstock particularities. Moreover, it should imply the study of mass and energy flows, as well as economic and environmental considerations and financial aspects. However, this research may be the starting point for considering what part of the natural detrital inorganic matter in biowastes may be an ally for their thermal valorisation.

4. Conclusions

The natural detrital inorganic matter of POW (carbonates of epiphytes, AAEM chlorides of marine salt, SiO_2 of sand, etc.) has a significant influence on its pyrolysis, not only on biopolymer degradation, but also on the formation and/or capture of certain pyrolytic compounds. Thus, the high concentrations of alkali metals accelerate the breakage of β-O-4 structures of lignin, hemicellulose degradation and promotes fragmentation reactions, HCOOH being produced in the range 250 °C–360 °C.

Also, alkali metals and Fe_2O_3 boost the release of atomic oxygen, especially from 500 °C. Thus, among other mechanisms, O may be formed by: (i) methyl (CH_3·) breakage from methoxy radicals (CH_3-O·) and (ii) Fe_2O_3 reduction with reducing pyrolysis gases such as CO. Through its participation in the formation of H_2SO_4 and sulphates, O may be partly responsible for retaining SO_2 and HCOOH formation.

At temperatures higher than 500 °C, carbonate decomposition together with the presence of AAEMs and Fe_2O_3 produce a series of reactions that have a remarkable impact on POW pyrolysis. Thus, the following effects are produced: (i) a negligible release of HCl and SO_2, despite the high content of Cl and relatively high of S in $POW_{unwashed}$ compared with other types of biomass; (ii) steam and CO_2 reforming of hydrocarbons and oxygenated compounds, H_2 being produced; (iii) the gasification of char mainly with the oxygen released, CO_2 and the steam formed; (iv) the significant release of HCOOH, which could be associated with the presence of NaOH and the formation of H_2SO_4; (v) the reverse of WGSR that reduces CO_2 and H_2 intensities and increases those of CO.

Thus, for the pyrolysis of POW, and depending on what is sought, not removing inorganic matter (marine salt, epiphytes, and sand) could be an interesting option, since the emission of undesirable compounds such as SO_2 and HCl is highly reduced and HCOOH formation is promoted. However, due to the great variability of detrital inorganic matter of POW depending on its origin, for optimizing its pyrolysis, a comprehensive characterization of the material is needed. Nevertheless, for a commercial application, further research considering the effect of inorganic matter on organic macromolecules decomposition is needed to stablish an adequate temperature and residence time for POW pyrolysis.

Funding sources

This research did not receive any specific grant from funding agencies in the public, commercial, or not-for-profit sectors.

CRediT authorship contribution statement

M.B. Folgueras: Conceptualization, Data curation, Formal analysis, Investigation, Methodology, Software, Supervision, Validation, Visualization, Writing – original draft, Writing – review & editing. **Antonio J. Gutiérrez-Trashorras:** Resources, Writing – review & editing. **G. Laine-Cuervo:** Investigation, Validation, Writing – review & editing. **Juan Carlos Ríos-Fernández:** Conceptualization, Data curation, Formal analysis, Investigation, Methodology, Project administration, Software, Validation, Visualization, Writing – original draft, Writing – review & editing.

Declaration of competing interest

The authors declare that they have no known competing financial interests or personal relationships that could have appeared to influence the work reported in this paper.

Data availability

No data was used for the research described in the article.

Appendix A. Supplementary material

Supplementary data to this article can be found online at https://doi.org/10.1016/j.wasman.2024.04.014.

References

Aires, T., Marbà, N., Cunha, R.L., Kendrick, G.A., Walker, D.I., Serrão, E.A., Duarte, C.M., Arnaud-Haond, D., 2011. Mar. Ecol. Prog. Ser. 421, 117–130. https://doi.org/10.3354/meps08879.

Akbari, M., Loganathan, N., Tavakolian, H., Mardani, A., Štreimikienė, D., 2021. Acta Montanistica Slovaca, 26(1), 1–17. doi: 10.46544/AMS.v26i1.01.

Anca-Couce, A., 2016. Prog. Energy Combust. Sci. 53, 41–79. https://doi.org/10.1016/j.pecs.2015.10.002.

Balata, G., Tola, A., 2018. J. Clean. Prod. 172, 4085–4098. https://doi.org/10.1016/j.jclepro.2017.02.072.

Bay, D., 1984. Aquat. Bot. 20 (1–2), 43–64. https://doi.org/10.1016/0304-3770(84)90026-3.

Bazargan, A., Kostić, M.D., Stamenković, O.S., Veljković, V.B., McKay, G., 2015. Fuel 150, 519–525. https://doi.org/10.1016/j.fuel.2015.02.046.
Bencoova, B., Grosos, R., Gomory, M., Bacova, K., Michalcova, S., 2021. Acta Montan. Slovaca 26, 139–148. https://doi.org/10.46544/AMS.v26i1.12.
Biagini, E., Barontini, F., Tognotti, L., 2006. Ind. Eng. Chem. Res. 45 (13), 4486–4493. https://doi.org/10.1021/ie0514049.
Bianchi, C.N., Bedulli, D., Morri, C., 1989. Occhipinti Ambrogi, A., L'herbier de Posidonies: écosystème ou carrefour éco-éthologique. In: Boudouresque, C.F., Jeudy de Grissac, A., Oliver, J. (Eds.), The first International Workshop on Posidonia oceanica beds. GIS Posidonie, Marseille, pp. 257–272.
Boletín Oficial de las Islas Baleares (BOIB), n° 12, January 26, 2023. Residuos sólidos urbanos. https://www.caib.es/eboibfront/es/2023/11687/.
Borum, J., Duarte, C.M., Krause-Jensen, D., Greve, T.M., 2004. European Seagrasses: An Introduction to Monitoring and Management.
Boudouresque, C.F., de Grissac, A.J., Olivier, J., 1984. International Workshop on Posidonia oceanica Beds: The First International Workshop on Posidonia Oceanica Beds. G.I.S. Posidonie, Marseille.
Boxiong, S., Qinlei, 2006. Energy Convers. Manag. 47, 1429–1437. https://doi.org/10.1016/j.enconman.2005.08.016.
Cagnon, B., Py, X., Guillot, A., Stoeckli, F., Chambat, G., 2009. Bioresour. Technol. 100, 292–298. https://doi.org/10.1016/j.biortech.2008.06.009.
Cebrian, J., Duarte, C.M., 2001. Aquat. Bot. 70(4), 295–309. https://www.sciencedirect.com/science/article/abs/pii/S0304377001001541?via%3Dihub#:~:text=https%3A//doi.org/10.1016/S0304%2D3770(01)00154%2D1.
Chen, H.D., Chen, X.L., Qiao, Z., Liu, H.F., 2016. Fuel 167, 31–39. https://doi.org/10.1016/j.fuel.2015.11.059.
Chen, X., Chen, Y., Yang, H., Chen, W., Wang, X., Chen, H., 2017. Bioresour. Technol. 233, 15–20. https://doi.org/10.1016/j.biortech.2017.02.070.
Chu, S., Subrahmanyam, A.V., Huber, G.W., 2013. Green Chem. 15, 125. https://doi.org/10.1039/C2GC36332A.
Cocozza, C., Parente, A., Zaccone, C., Mininni, C., Santamaria, P., Miano, T., 2011. Waste Manag. 31 (1), 78–84. https://doi.org/10.1016/j.wasman.2010.08.016.
Dasgupta, K., Rai, K., Verma, N., 2003. Can. J. Chem. Eng. 81, 53–62. https://doi.org/10.1002/cjce.5450810106.
David, W.T., Rounthwaite, C., Carpenter, N., 1948. Nat. 161, 726. https://doi.org/10.1038/161726a0.
De Falco, G., Simeone, S., Baroli, M., 2008. Management of beach-cast Posidonia oceanica seagrass on the island of Sardinia (Italy, Western Mediterranean). J. Coast. Res. 24, 69–75. https://doi.org/10.2112/06-0800.1.
Debiagi, P.E.A., Pecchi, C., Gentile, G., Frassoldati, A., Cuoci, A., Faravelli, T., Ranzi, E., 2015. Energy Fuels 29, 6544–6555. https://doi.org/10.1021/acs.energyfuels.5b01753.
Demirbas, A., Güllü, D., Caglar, A., Akdeniz, F., 1997. Energy Source. 19 (8), 765–770. https://doi.org/10.1080/00908319708908888.
Di Blasi, C., 2008. Prog. Energy Combust. Sci. 34 (1), 47–90. https://doi.org/10.1016/j.pecs.2006.12.001.
European Council. Council Directive 92/43/EEC of 21 May 1992 on the conservation of natural habitats and of wild fauna and flora. https://eur-lex.europa.eu/legal-content/EN/TXT/HTML/?uri=CELEX:31992L0043.
Fahim, M.A., Al-Sahhaf, T.A., Elkilani, A., 2010. Fundam. of Petroleum Refin. Elsevier B. V. doi: 10.1016/C2009-0-16348-1.
Fahmi, R., Bridgwater, A.V., Darvell, L.I., Jones, J.M., Yates, N., Thain, S., Donnison, I.S., 2007. Fuel 86, 1560–1569. https://doi.org/10.1016/j.fuel.2006.11.030.
Faravelli, T., Frassoldati, A., Migliavacca, G., Ranzi, E., 2010. Biomass Bioenergy 34, 290–301. https://doi.org/10.1016/j.biombioe.2009.10.018.
Folgueras, M.B., Gómez-Martín, J.M., Diez, M.A., 2023. J. Anal. Appl. Pyrolysis 169, 105861. https://doi.org/10.1016/j.jaap.2023.105861.
Gambi, M.C., Hall-Spencer, J.M., Cigliano, M., Cocito, S., Lombardi, C., Lorenti, M., Patti, F.P., Porzio, L., Rodolfo-Metalpa, R., Buia, M.C., 2010. Biol. Mar. Mediterr. 17, 86–88. http://hdl.handle.net/10026.1/1413.
Gazeau, F., Duarte, C.M., Gattuso, J.-P., Barrón, C., Navarro, N., Ruiz, S., et al., 2005. Biogeosciences 2 (1), 43–60. https://doi.org/10.5194/bg-2-43-2005.
Green, P., Short, F.T, 2003. World Atlas of Seagrasses, Prepared by UNEP World Conservation Monitoring Centre, University of California Press, Berkeley.
Hietala, J., Vuori, A., Johnsson, P., Pollari, I., Reutemann, W., Kieczka, H., 2016. Formic acid. Ullmann's encyclopedia of industrial chemistry, 1 1–22. .
Hough, B.R., Schwartz, D.T., Pfaendtner, J., 2016. Ind. Eng. Chem. Res. 55 (34), 9147–9153. https://doi.org/10.1021/acs.iecr.6b02092.
Hu, S., Jiang, L., Wang, Y., Su, S., Sun, L., Xu, B., He, L., Xiang, J., 2015. Bioresour. Technol. 192, 23–30. https://doi.org/10.1016/j.biortech.2015.05.042.
Hu, B., Lu, Q., Jiang, X., Dong, X., Cui, M., Dong, C., Yang, Y., 2018. J. Energy Chem. 27 (2), 486–501. https://doi.org/10.1016/j.jechem.2017.11.013.
Hu, Q., Shen, Y., Chew, J.W., Ge, T., Wang, C.-H., 2020. Chem. Eng. J. 379, 122346 https://doi.org/10.1016/j.cej.2019.122346.
Iáñez-Rodríguez, I., Martín-Lara, M.Á., Blázquez, G., Osegueda, Ó., Calero, M., 2019. J. Energy Chem. 32, 105–117. https://doi.org/10.1016/j.jechem.2018.07.002.
Idriss, H., Seebauer, E.G., 2000. Reactions of ethanol over metal oxides. J. Mol. Catal. A Chem. 152, 201–212. https://doi.org/10.1016/S1381-1169(99)00297-6.
Jiménez, S., Cano, R., Bayle, J., Ramos, A., Sánchez, J.L., 1996. Las praderas de Posidonia oceanica (L.) Delile como zona de protección de juveniles de especies de interés comercial. In: Perejón, A. (Ed.), Real Sociedad Española de Historia Natural: tomo extraordinario publicado con motivo del 125 aniversario de su fundación. Real Sociedad Española de Historia Natural, Madrid, pp. 375–378.
Kaal, J., Serrano, O., del Río, J.C., Rencoret, J., 2018. Org Geochem. 124, 247–256. https://doi.org/10.1016/j.orggeochem.2018.07.017.
Khiari, R., Mhenni, M.F., Belgacem, M.N., Mauret, E., 2010. Bioresour. Technol. 101, 775–780. https://doi.org/10.1016/j.biortech.2009.08.079.
Kim, K.H., Eom, I.Y., Lee, S.M., Choi, D., Yeo, H., Choi, I.-G., Choi, J.W., 2011. J. Anal. Appl. Pyrolysis 92 (1), 2–9. https://doi.org/10.1016/j.jaap.2011.04.002.
Kraiem, T., Hassen, A.B., Belayouni, H., Jeguirim, M., 2017. Environ. Sci. Pollut. Res. 24, 9951–9961. https://doi.org/10.1007/s11356-016-7704-z.
Kwon, S., Chae, H.-J., Na, K., 2020. Catal. Today 352, 111–117. https://doi.org/10.1016/j.cattod.2020.01.014.
Li, S., Calmels, D., Han, G., Gaillardet, J., Liu, C., 2008. Earth Planet. Sci. Lett. 270, 189–199. https://doi.org/10.1016/J.EPSL.2008.02.039.
Li, S., Wang, C., Luo, Z., Zhu, X., 2020. Energy Fuels 34 (10), 12654–12664. 10.1021/acs.energyfuels.0c01938.
Maisano, S., Urbani, F., Cipitì, F., Freni, F., Chiodo, V., 2019. Syngas production by BFB gasification: experimental comparison of different biomasses. Int. J. Hydrogen Energy 44 (9), 4414–4422. https://doi.org/10.1016/j.ijhydene.2018.11.148.
Marošek, J., 2013a. Clean Techn. Environ. Policy 15, 721–725. https://doi.org/10.1007/s10098-012-0549-3.
Marošek, J., Gavurová, B., 2022. Chemosphere 291, 1330088. https://doi.org/10.1016/j.chemosphere.2021.133008.
Marošek, J., Itoh, S., Higa, O., Kondo, Y., Ueno, M., Suwa, R., Kawamitsu, Y., 2013b. J. Chem. Technol. Biotechnol. 88 (9), 1650–1653. https://doi.org/10.1002/jctb.4014.
Marošek, J., Minofar, B., Marošková, A., Strunecký, O., Gavurová, B., 2023a. Environ. Technol. Innov. 30, 103109 https://doi.org/10.1016/j.eti.2023.103109.
Marošek, J., Gavurová, B., Strunecký, O., Marošková, A., Sekar, M., Marek, V., 2023b. Fuel 344, 128056. https://doi.org/10.1016/j.fuel.2023.128056.
Marošek, J., Marošková, A., Gavurová, B., Minofar, B., 2023c. J. Clean. Prod. 412, 137326 https://doi.org/10.1016/j.jclepro.2023.137326.
Mendu, V., Harman-Ware, A.E., Crocker, M., Jae, J., Stork, J., Morton, S., Placido, A., Huber, G., DeBolt, S., 2011. Biotechnol. Biofuels 4, 43. https://doi.org/10.1186/1754-6834-4-43.
Moltó, J., Montalbán, M.G., Núñez, S.S., Jordá, J.D., 2022. Appl. Sci. 12 (15), 7422 https://doi.org/10.3390/app12157422.
Nash, M., Opdyke, B., Troitzsch, U., et al., 2013. Nat. Clim. Change 3, 268–272. https://doi.org/10.1038/nclimate1760.
Neven, V., Mateja, G., Anamarija, P., Tajana, K., 2019. Bioenergy Res. 12, 1104–1112. https://doi.org/10.1007/s12155-019-10032-7.
Otun, K.O., Liu, X., Hildebrandt, D., 2020. J. Energy Chem. 51, 230–245. https://doi.org/10.1016/j.jechem.2020.03.062.
Pasqualini, V., Pergent-Martini, C., Clabaut, P., Pergent, G., 1998. Estuar. Coast. Shelf Sci. 47 (3), 359–367. https://doi.org/10.1006/ecss.1998.0361.
Pavolova, H., Bakalár, T., Kysel'a, K., Klimek, M., Hajduova, Z., Zawada, M., 2021. Acta Montanistica Slovaca, 26(1), 161–170. doi: 10.46544/AMS.v26i1.14.
Peng, B., Li, X., Luo, J., Yu, X., 2019. Energy Fuels 33, 9272–9279. https://doi.org/10.1021/acs.energyfuels.9b02097.
Peterson, K.M., Heaney, P.J., Post, J.E., 2018. Powder Diffr. 33 (4), 287–297. https://doi.org/10.1017/S0885715618000623.
Pilavtepe, M., Celiktas, M.S., Sargin, S., Yesil-Celiktas, O., 2013. Ind. Crop. Prod. 51, 348–354. https://doi.org/10.1016/j.indcrop.2013.09.020.
Rahim, M.U., Gao, X.P., Garcia-Perez, M., Li, Y., Wu, H.W., 2013. Energy Fuels 27 (1), 310–317. https://doi.org/10.1021/ef3018157.
Romero, J., 2004. La producción primaria y su destino. Características de los restos de la planta. In: Luque, A.A., Templado, J. (Coords.), Praderas y bosques marinos de Andalucía: Las praderas de Posidonia, Junta de Andalucía, Consejería de medio ambiente. Sevilla, pp. 74–81.
Rong, L., Xu, Z., Sun, J., Guo, G., 2018. J. Energy Chem. 27 (1), 238–242. https://doi.org/10.1016/j.jechem.2017.07.015.
Ruipérez, M., Salazar, J. M., Alarcón, D., Verborgh, P., Meizoso, M. J., de Stephanis, R., Posidonia: la joya del Mediterráneo. Publicación divulgativa sobre las praderas de Posidonia oceanica. Proyecto LIFE09 NAT/ES/000534, Circe, Algeciras, 2012.
Saleh, S.B., Flensborg, J.P., Shoulaifar, T.K., Sárossy, Z., Hansen, B.B., Egsgaard, H., DeMartini, N., Jensen, P.A., Glarborg, P., Dam-Johansen, K., 2014. Energy Fuels 28 (6), 3738–3746. https://doi.org/10.1021/ef4021262.
Sebio-Puñal, T., Naya, S., López-Beceiro, J., Tarrió-Saavedra, J., Artiaga, R., 2012. J. Therm. Anal. Calorim. 109, 1163–1167. https://doi.org/10.1007/s10973-011-2133-1.
Shen, C., Azevedo, J.L.T., 2005. Biomass Bioenergy 28, 499–507. https://doi.org/10.1016/j.biombioe.2004.11.008.
Shoja, M., Babatabar, M.A., Tavasoli, A., Ataei, A., 2013. J. Energy Chem. 22 (4), 639–644. https://doi.org/10.1016/S2095-4956(13)60084-4.
Simeone, S., 2008. J. Coast. Res. 65, 1045–1050. https://dspace.unitus.it/bitstream/2067/2054/1/ssimeone_tesid.pdf.
Stávková, A., Marošek, J., 2021. Chemosphere 276. https://doi.org/10.1016/j.chemosphere.2021.130097.
Terrados J., Duarte, C.M., 2000. J. Ex. Mar. Biol. Ecol. 243(1), 45–53. doi: 10.1016/S0022-0981(99)00110-0.
Usachev, N.Y., Krukovskii, I.M., Kanaev, S.A., 2004. Petroleum Chem. 44 (6), 411–427.
Usino, D.O., Supriyanto, Ylitervo, P., Pettersson, A., Richards, T., 2020. J. Anal. Appl. Pyrolysis 147, 104782. https://doi.org/10.1016/j.jaap.2020.104782.
Vassilev, S.V., Baxter, D., Andersen, L.K., Vassileva, C.G., Morgan, T.J., 2012. Fuel 94, 1–33. https://doi.org/10.1016/j.fuel.2011.09.030.
Vassilev, S.V., Baxter, D., Vassileva, C.G., 2013. Fuel 112, 391–449. https://doi.org/10.1016/j.fuel.2013.05.043.
Wang, S., Dai, G., Yang, H., Luo, Z., 2017. Prog. Energy Combust. Sci. 62, 33–86. https://doi.org/10.1016/j.pecs.2017.05.004.

Wang, W., Lemaire, R., Bensakhria, A., Luart, D., 2022. J. Anal. Appl. Pyrolysis 163, 105479. https://doi.org/10.1016/j.jaap.2022.105479.
Wang, S.-R., Liang, T., Ru, B., Guo, X.-J., 2013. Chem. Res. Chin. Univ. 29, 782–787. https://doi.org/10.1007/s40242-013-2447-6.
Widyawati, M., Church, T.L., Florin, N.H., Harris, A.T., 2011. Int. J. Hydrog. Energy 36 (8), 4800–4813. https://doi.org/10.1016/j.ijhydene.2010.11.103.
Yin, C.-Y., 2011. Fuel 90, 1128–1132. https://doi.org/10.1016/j.fuel.2010.11.031.
Zaafouri, K., ben Hassen Trabelsi, A., Krichah, S., Ouerghi, A., Aydi, A., Clapman, C.A., et al., 2016. Bioresour. Technol. 207, 387–398. https://doi.org/10.1016/j.biortech.2016.02.004.